# RSC Advances

ROYAL SOCIETY
OF CHEMISTRY

www.rsc.org/advances
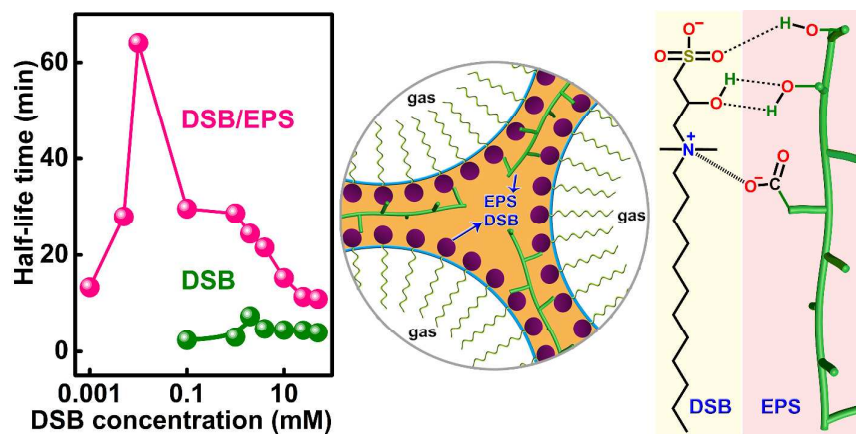
Weak hydrogen bonding and electrostatic interactions between a zwitterionic surfactant

dodecyl sulfobetaine (DSB) and a hyperbranched exopolysaccharide (EPS) enhanced

considerably the stability and foamability of EPS/DSB foam.

1    **Enhancement of foamability and foam stability induced by**

2    **interactions between a hyperbranched exopolysaccharide and a**

3    **zwitterionic surfactant dodecyl sulfobetaine**

4

5    **Quanhua Deng[a], Haiping Li[b], Chunxiu Li[a], Weiqin Lv[a], Ying Li[a]\***

6

7    *[a]Key Laboratory for Colloid and Interface Chemistry of Education Ministry, Shandong*

8    *University, Jinan 250100, P.R. China;*

9    *[b]National Engineering Technology Research Center for Colloidal Materials,*

10   *Shandong University, Jinan 250100, P.R. China;*

11
12
13

14

15

16

17

18           [*] To whom correspondence should be addressed

19               Email: yingli@sdu.edu.cn

20               Telephone: +86-531-88362078

21               Fax: +86-531-88362078

22

23

24
25
26
27
28   **Running title:** Enhancement of foamability and foam stability

## Abstract

An aqueous foam containing a zwitterionic surfactant dodecyl sulfobetaine (DSB) and an eco-friendly hyperbranched exopolysaccharide (EPS) secreted by a deep-sea mesophilic bacterium *Wangia profunda* SM-A87 was prepared for the first time. Compared with singular DSB solution, the EPS/DSB mixing solution exhibited better foamability and foam stability. The minimum DSB concentration ($C_{DSB}$) needed to form a stable foam in the EPS/DSB solution was about one hundred times that in the DSB solution, and in a very large $C_{DSB}$ range, the EPS/DSB foam exhibited a better stability. The enhancement of foamability and foam stability of the complex solution arises from the hydrogen bonding and electrostatic interactions between the EPS and the DSB, and the hyperbranched structure of the EPS. The EPS/DSB foam shows great potential for application in enhanced oil recovery and health-care products.

## 1. Introduction

Aqueous foams have been applied in many fields, such as firefighting, pharmaceutical, mineral floatation, food processing, cosmetic and oil exploitation.[1, 2] Surfactants are the most extensively used foam stabilizers because of their ability of adsorbing at interfaces and lowering the interfacial energy of solutions. Nonetheless, the stability of surfactant foams is not always satisfactory. The coalescence and rupture of bubbles could not be avoided and were generally intensified along with the drainage of the foam film.[3] Up to now, it's still a technical challenge to obtain aqueous foam exhibiting long-term stability and high foamability, especially with a little dosage of surfactants.

Polyelectrolytes (PE) are often associated with surfactants to control the rheological properties of foams and enhance the foam stability.[4] According to the literature, oppositely charged PE and surfactant complex foams with suitable PE/surfactant concentration ratio could have high stability because of the co-adsorption of the PE and surfactants at air/water interfaces[5] driven by strong interactions between them. Unfortunately, the strong interactions caused a bad foamability of the complex solutions.[6, 7] Recently, some studies about PE/surfactant complex foams with weak interactions between the PE and surfactants were reported, such as the poly(vinylamine)/$C_{12}$TAB foam.[6] The synergy between the PE and the surfactants led to a fast surfactant adsorption on the solution surface which facilitated foaming of solutions, and the formed surface-active surfactant/PE complex, especially stiff PE/surfactant complex caused a strong steric repulsion, favorable for the

67   enhancement of foam stability.[8]

68   However, most of traditional PE[9-12] are toxic or would bring about environmental

69   contamination. Developing eco-friendly macromolecules such as polysaccharides and

70   proteins satisfies the requirements of sustainable development. Compared with

71   proteins, polysaccharides are of much lower cost and easier to be obtained,[13-17] and

72   some of them possess excellent rheological and interfacial adsorption properties,

73   which renders them suitable for enhancing the foamability and foam stability.[18, 19]

74   Lately, a low-cost hyperbranched exopolysaccharide (EPS) secreted from a

75   deep-sea mesophilic bacterium *Wangia profunda* SM-A87[20, 21] has attracted much

76   attention of researchers because of its strong thickening ability and excellent salt and

77   pH resistance.[22, 23] EPS molecules contain hydroxyl, hemiacetal, and carboxyl groups,

78   which brings about the possibility that the EPS interacts with surfactants to enhance

79   their foamability and foam stability. Nonetheless, no research on EPS/surfactant

80   foams has been reported.

81   In this study, an aqueous foam containing the EPS and a widely used zwitterionic

82   surfactant[24-28] dodecyl sulfobetaine (DSB) was firstly prepared. The EPS/DSB foam

83   presented much better foamability and foam stability than the DSB foam. Related

84   mechanisms were discussed thoroughly. This work provides a deep insight into the

85   mechanism of performance enhancement of PE/surfactant complex foam with weak

86   interactions, and a very useful approach to exploring eco-friendly high efficient foams.

87   The EPS/DSB foam has great application potential in enhanced oil recovery and

88   detergent areas.

89 **2. Experimental**

90 *2.1. Materials*

91     SM-A87 EPS was prepared by the method reported in the literature.[21] Its

92 weight-average molecular weight is ~$3.76 \times 10^6$ g/mol. The glycosyl composition and

93 linkage analyses of EPS were reported previously.[23] Dodecyl sulfobetaine (DSB,

94 analytical pure) was synthesized and purified by Jin Ling Petrochemical Co., Ltd. (P.R.

95 China). Ultra-pure water obtained from a Hitech-Kflow water purification system (P.R.

96 China) was used in this work.

97 *2.2. Preparation of solutions*

98     EPS stock solutions (3 g/L) were prepared by dissolving 0.3 g of EPS in 100 mL

99 of water. The concentration of DSB stock solution was 100 mM. Solutions with low

100 concentrations were obtained *via* dilution of the stock solutions. EPS concentration

101 ($C_{EPS}$) is 1.5 g/L in all experiments unless special explanation.

102 **2.3. Methods**

103 *2.3.1. Static foam properties*

104     Foam properties of all the solutions were characterized using an IT Concept

105 Foamscan instrument (Teclis Co., France). Foam was generated by blowing nitrogen

106 through a porous glass filter with a blowing rate of 75 mL/min. The initial solution

107 and final foam volumes were 60 and 200 mL, respectively. The half-life time ($t_{1/2}$) is

108 the time that the foam takes to decrease 50% of the volume. This parameter was used

109 to characterize the foam stability. The variation of foam volume with time displays the

110 drainage process.

111    ***2.3.2. Rheological properties of foams and bulk solutions***

112    The dynamic foam stability was measured using an external rotor disturbing

113    method.[29] The foam with total volume of 180 mL and gas volume percentage of ~78%

114    was *in situ* generated in a transparent glass bucket connected with a constant

115    temperature water bath by blowing $N_2$ gas bubbles at a constant flow rate of 0.01

116    L/min through a porous filter placed at the bottom of the solution with volume of 40

117    mL. Temperature was kept at $50 \pm 0.1$ °C. The dynamic $t_{1/2}$ and viscosity of the foam

118    were recorded by a Brookfield RS plus rheometer with a paddle rotor (Brookfield

119    Engineering Laboratories, Middleboro, USA).

120    Dynamic viscoelastic measurements of the foams were performed on an Anton

121    Paar MCR 302 rheometer (Austria) equipped with a paddle-shaped ST22-4V-40 rotor

122    at 50 °C. The wet foam was obtained by stirring 100-mL solutions using waring

123    blender (1500 mL) with a rate of 1000 r/min. The linear viscoelastic regions of the

124    foams were determined through stress sweep (0.01–10 Pa) at frequency of 1 Hz. The

125    variation of moduli with time was measured at frequency of 1 Hz and stress of 0.02

126    Pa until the rotor was exposed.

127    Rheological measurements of the bulk solutions were carried out on the MCR

128    302 rheometer with a CC27 coaxial cylinder measuring system at 50 °C. Steady shear

129    measurements were performed with shear rate increasing from 0.01 to 100 $s^{-1}$. For

130    dynamic viscoelastic measurements, the linear viscoelastic regions of solutions were

131    determined *via* stress sweep (0.01–10 Pa) at frequency of 0.5 Hz. The frequency

132    sweep was carried out from 0.01 to 5 Hz at stress of 0.02 Pa (in the linear viscoelastic

133    region).

### 2.3.3. Surface tension and interfacial dilational viscoelasticity

135    Dynamic surface tension and interfacial dilational modulus measurements were

136    performed on a Tracker oscillating bubble rheometer (Teclis Co., France) using the

137    pendant drop method. The surface tension relaxation kinetics after a pendant drop was

138    formed rapidly on the capillary tip, was followed for 1800 s until the equilibrium

139    surface tension was obtained. The drop was filmed by a CCD camera and the drop

140    profile was obtained using the image analysis software Optimas 6.5. The dilational

141    elasticity of the gas/water interfacial layer were determined at an oscillatory

142    frequency of 0.1 Hz. This method allows us to obtain the surface tension ($\gamma$) as well as

143    the area of the surface element ($A$) in the whole test process. Dilational surface moduli

144    are defined as the differential ratio of the $\gamma$ to $\ln A$.

145    $$\varepsilon = \frac{d\gamma}{d\ln A} \tag{1}$$

146    The surface area of the drop is oscillated periodically. The dilatational modulus is the

147    summation of elastic component ($\varepsilon_d$) and loss modulus ($\omega \eta_d$). $\varepsilon_d$ and $\omega \eta_d$ account for

148    recoverable energy stored in the interface and dissipation energy through relaxation

149    process, respectively. $\eta_d$ is the dilational viscosity.

150    $$\varepsilon = \varepsilon_d + i\omega \eta_d \tag{2}$$

151    $$\varepsilon_d = |\varepsilon|\cos\theta \tag{3}$$

152    $$\eta_d \omega = |\varepsilon|\sin\theta \tag{4}$$

153    where $|\varepsilon|$ is the absolute modulus and $\theta$ is the phase angle.

### 2.3.4. Texture analyze

155    The microhardness and the viscoelastic feature of foams were investigated with a

156    TMS-Pilot texture analyzer (TL-Pro testing system, FTC, USA).[29] Initially, a

157    cylindrical cell (150 mm inner diameter) was fullfilled with a known volume of wet

158    foam and placed on the sample platform. The wet foam was obtained by stirring

159    100-mL solutions using waring blender (1500 mL) at 1000 r/min. Then, the extrusion

160    disk with diameter of 100 mm was controlled by the computer workstation to depress

161    the foam at a constant speed of 20 mm/min. When the extrusion disk moves through

162    the set distance, it went backward to its departure place. Over the whole process,

163    pressures at the bottom and side of the disk were recorded. The maximum

164    compressing force and viscoelastic force indicate the compressing and dragging peak

165    pressures in the falling and pulling procedures which qualitatively correspond to the

166    stiffness and the viscoelasticity of the foam, respectively.

167    ***2.3.5 Fourier transform infrared (FT-IR) spectrum and microscope observation***

168    FT-IR spectrum of samples were obtained on a VERTEX-70/70 V FT-IR

169    spectrometer (Bruker Optics, Germany) using KBr tablet method. Each spectrum was

170    recorded in the range of 4000–400 $cm^{-1}$ with resolution of 4 $cm^{-1}$. EPS/DSB complex

171    was obtained by drying their mixing solutions at 60 °C.

172    Images of foam bubbles were photographed by a BX53 microscope (Olympus,

173    Japan). 50 mL of DSB and EPS/DSB solutions with $C_{EPS}$ of 0.75 g/L and $C_{DSB}$ of 2

174    mM were stirred by a waring blender (1500 mL) at 1000 r/min for 1 min to obtained

175    wet foam. Then the wet foam was transferred immediately into a quatz sample cell

176    with thickness of 1 mm and observed using the microscope.

177    *2.3.6 Microthermal analysis*

178    A micro-differential scanning calorimeter (DSC) (Rheometric Scientific Inc., USA)

179    was used to determine thermal properties of solutions. The scanning rate was

180    2 °C/min during the thermal cycle of heating to cooling from -20–20 °C. The

181    reference cell was filled with water.

182    **3. Results and discussion**

183    *3.1. Foamability and foam stability of DSB and EPS/DSB solutions*

184    Foaming time ($t_f$), the time taken to form specific volume of foam, which is an

185    important parameter reflecting the foaming capability of solutions. A shorter $t_f$ means

186    a better foamability.[30] Fig. 1a shows the variation of the $t_f$ of DSB and EPS/DSB

187    solutions as a function of $C_{DSB}$. For pure DSB solutions, foams were not formed at

188    $C_{DSB}$ < 0.1 mM. At $C_{DSB}$ > 0.1 mM, the $t_f$ decreases with increasing $C_{DSB}$, and keeps

189    almost constant at $C_{DSB}$ > 2.0 mM in which range the DSB adsorption at the interface

190    gets saturated.[31] For EPS/DSB solutions, foams can be formed at much lower $C_{DSB}$

191    (0.001 mM), and the $t_f$ first decreases, followed by an increase, and then decreases

192    with increasing $C_{DSB}$. At $C_{DSB}$ < 2 mM, the $t_f$ of the EPS/DSB solutions are much less

193    than that of the corresponding DSB solutions.

194    According to the DSC results (Fig. S1, Supporting information), the freezing

195    point of water decreases obviously after the addition of EPS, which probably stems

196    from the EPS induced polarity increase of the water, just like the effect of ionic

197    strength.[4, 32, 33] The increase of water polarity can result in the increase of interfacial

198    adsorption tendency of DSB molecules and thus the reduced $t_f$ at $C_{DSB}$ < 2 mM or >

199    10 mM. At 2 mM < $C_{DSB}$ < 10 mM, the $t_f$ of the EPS/DSB solutions increases with

200    increasing $C_{DSB}$, and is even larger than that of the corresponding DSB solutions,

201    which is probably related to the reduction of the DSB adsorption tendency at the

202    interface because of the formation of EPS/DSB aggregates in the bulk solutions.[6]
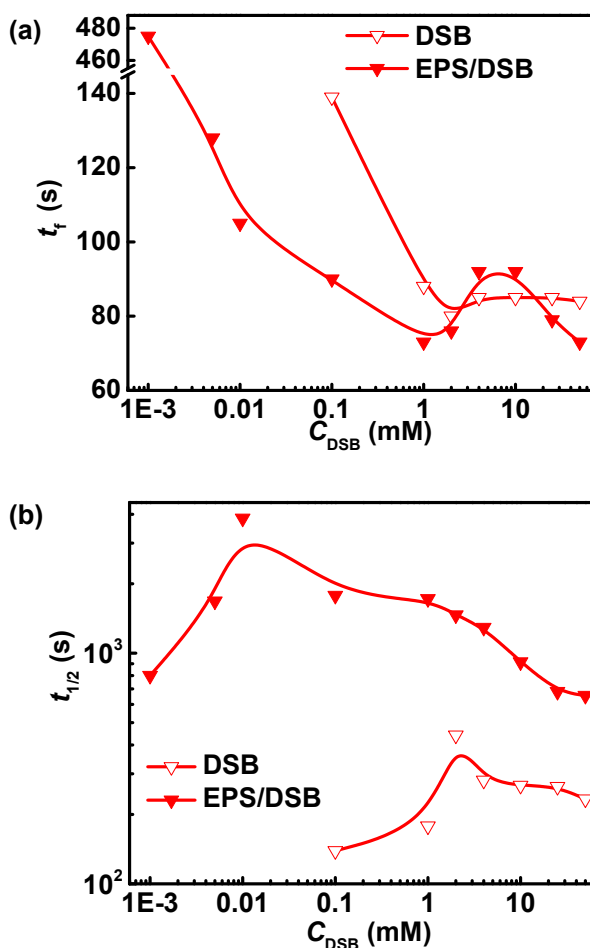


203

204

205    **Fig. 1** (a) Foaming time and (b) foam stability of DSB and EPS/DSB solutions with

206    $C_{EPS}$ of 1.5 g/L and different $C_{DSB}$.

207

208         Foam stability, one of the most important characteristics of aqueous foam,

209    depends on many factors, such as drainage of foam films, bulk viscosity of solutions,

210    interfacial elasticity,[34] diffusion of gas through foam film,[35-37] and steric[38] and

electrostatic repulsion between the two sides of foam films.[39] The $t_{1/2}$ is usually used

to evaluate the stability of foams.[40] Fig. 1b shows the change of $t_{1/2}$ of DSB and

EPS/DSB foams with $C_{DSB}$. For pure DSB solutions, the $t_{1/2}$ increases gradually,

reaches the maximum at $C_{DSB}$ = 2.0 mM, and then decreases slightly with increasing

$C_{DSB}$, which coincides with the normal trend of common surfactant foams.[41] In the

investigated $C_{DSB}$ range, the $t_{1/2}$ of the EPS/DSB foams is much larger than that of the

DSB foams. At $C_{DSB}$ = 0.1 mM, the $t_{1/2}$ of the EPS/DSB foam is more than 12 times

that of the DSB foam. At $C_{DSB}$ < 0.1 mM, no stable foam was formed from the DSB

solution, but the $t_{1/2}$ of the EPS/DSB foams can reach several hours. To find out how

the foamability and foam stability of the EPS/DSB solutions are enhanced so

markedly, the interfacial and bulk phase characteristics of the complex solutions were

studied.

### *3.2 Bulk and interfacial rheology of EPS/DSB solutions*
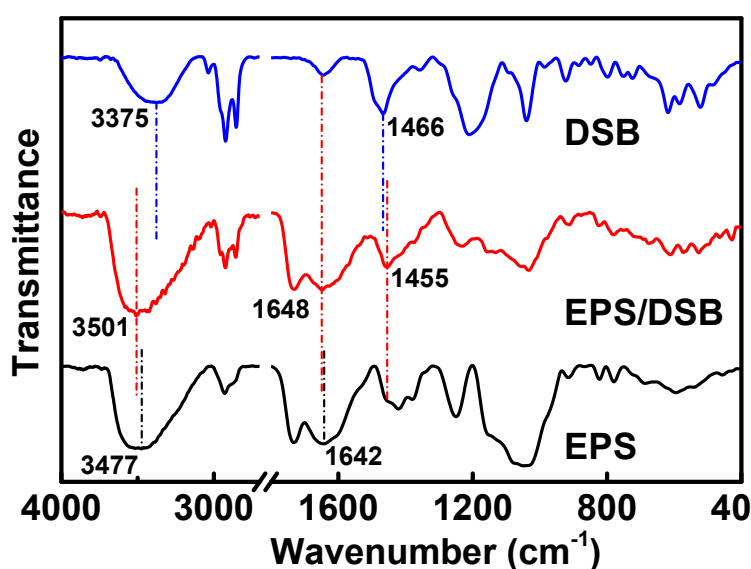


**Fig. 2** FT-IR spectra of DSB, EPS and EPS/DSB composites with DSB mass percent

of 80%.

227

228     Intermolecular interactions considerably affect the rheological properties of their

229     solutions.[42, 43] The FT-IR spectra of EPS, DSB and EPS/DSB composite were

230     measured to characterize interactions between the EPS and the DSB. As shown in Fig.

231     2, the peaks of EPS at 3477 $cm^{-1}$, DSB at 3375 $cm^{-1}$ and EPS/DSB composite at 3501

232     $cm^{-1}$ are ascribed to the stretching vibration of O-H.[44] An obvious blue shift of the

233     O-H absorption peak of the composite is observed, and it's probably induced by the

234     hydrogen bonding interaction between the EPS and the DSB (Scheme 1) which

235     destroys the intermolecular hydrogen bonds[45] of the EPS. The peaks of EPS at 1642

236     $cm^{-1}$ and DSB at 1466 $cm^{-1}$ are ascribed to the asymmetric stretching vibration of –

237     $COO^-$ [46] and $C-N^+$ stretching vibration,[47] and they shift to 1648 and 1455 $cm^{-1}$ in the

238     EPS/DSB composite, respectively, probably due to the electrostatic attractive

239     interaction between $-COO^-$ and $N^+$ (Scheme 1). Therefore, the EPS interacts with the

240     DSB $via$ the hydrogen bonds and the electrostatic attraction force.



241
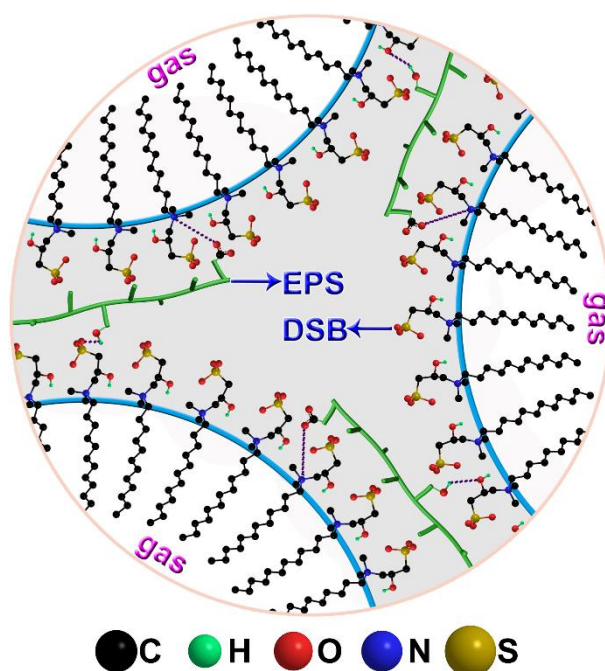
242    **Scheme 1** Schematic illustrations for Plateau borders of EPS/DSB foam. Dotted lines

243    in the scheme denote hydrogen bonds and electrostatic interaction between EPS and

244    DSB molecules.

245

246    The equilibrium surface tension obtained from dynamic surface tension curves of

247    DSB and EPS/DSB solutions with $C_{EPS}$ of 1.5 g/L at different $C_{DSB}$ (Fig. S2,

248    Supporting information) are shown in Fig. 3a. The surface tensions of both the DSB

249    and EPS/DSB solutions decrease with increasing $C_{DSB}$ until reaching an equilibrium.

250    At $C_{DSB}$ < 0.1 mM, the equilibrium surface tension of the EPS/DSB solutions is

251    obviously lower than that of the corresponding DSB solutions, which is ascribed to

252    that the EPS strengthens the interfacial adsorption tendency of DSB (agreeing well

253    with the results in Fig. 1a), and that the EPS/DSB complex was formed *via* the

254    hydrogen bonds and electrostatic force at the interface. At $C_{DSB}$ > 2.0 mM, the surface

255    tension of EPS/DSB solutions was higher than that of relative DSB solutions. This

256    results from the coaggregation of EPS and DSB micelles in the bulk solutions which

257    reduces the interfacial adsorption amount of DSB molecules.[48]



258

259
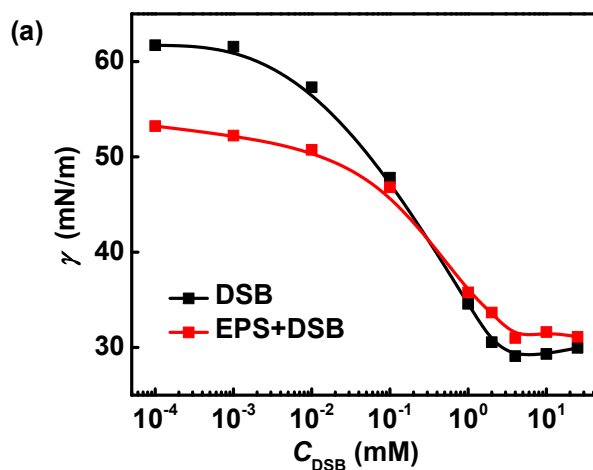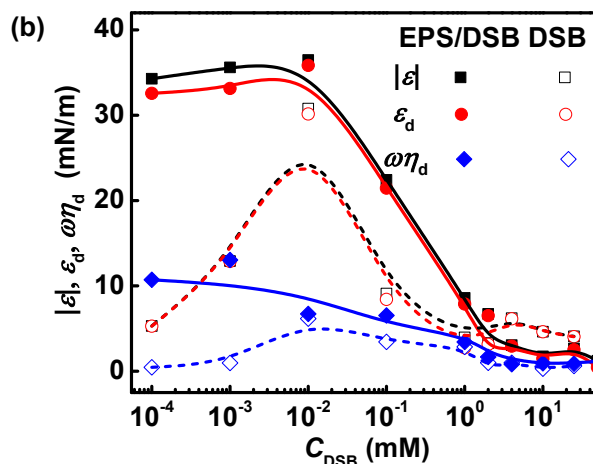
**Fig. 3** (a) Surface tension ($\gamma$) and (b) interfacial dilational viscoelasticity of DSB and EPS/DSB solutions as a function of $C_{DSB}$ with $C_{EPS}$ of 1.5 g/L at 25 °C. $|\varepsilon|$, absolute modulus; $\varepsilon_d$, dilational elasticity; $\omega\eta_d$, dilational viscous component.

263

As reported, the interfacial dilational elasticity of surfactant solutions was very sensitive to the variation of the interfacial composition. It's an important factor influencing the drainage, Ostwald ripening, coalescence processes, and then the stability of foams.[49-51] As shown in Fig. 3b, the absolute modulus ($|\varepsilon|$) and dilational elasticity ($\varepsilon_d$) of the surface layer of pure DSB solution both initially increase with increasing $C_{DSB}$ at $C_{DSB}$ < 0.01 mM, which is ascribed to the increasing interfacial adsorption amount[8] of DSB, and consequently decrease at $C_{DSB}$ > 0.01 because of the reduction of the $C_{DSB}$ difference between the interface and the bulk solutions, and the increasing diffusion rate of DSB molecules from the bulk solutions to the interface.

$|\varepsilon|$ and $\varepsilon_d$ of the EPS/DSB solutions are much larger at very low $C_{DSB}$ compared with corresponding DSB solutions, which, on one hand, demonstrates that the interfacial adsorption tendency of the DSB is strengthened by the EPS and, on the

276      other hand, hints that the EPS molecules probably integrate with DSB molecules at

277      the interface. The EPS molecules can interact with each other through hydrogen

278      bonds to form gel-like networks in the bulk phase,[23] and the hyperbranched structure

279      of EPS molecules prohibits the molecular curling and thus ensures the relatively

280      larger hydrodynamic radium and more interacting sites with the DSB molecules,[20, 21]

281      so the EPS network would combine with the DSB molecules at the interface,

282      substantially increasing the structural strength of foam films. At $C_{DSB} > 2.0$ mM, the

283      formation of the EPS/DSB aggregates induces the depletion of the DSB molecules at

284      the interface, so the $|\varepsilon|$ and $\varepsilon_d$ of the complex solutions are lower than those of the

285      relative DSB solutions.

286          In Fig. 3b, the $\varepsilon_d$ is much greater than the corresponding $\omega\eta_d$, revealing a

287      dominant elastic character of the DSB interfacial layer. The $|\varepsilon|$, $\varepsilon_d$ and $\omega\eta_d$ of the

288      EPS/DSB complex solutions are much larger than those of the relative pure DSB

289      solutions at $C_{DSB} < 2$ mM, and the maximums of $|\varepsilon|$ and $\varepsilon_d$ appear at $C_{DSB}$ of ~0.01

290      mM exactly when the EPS/DSB foam exhibits the best stability (Fig. 1b), which

291      suggests that the EPS induced enhancement of the interfacial elasticity of the

292      EPS/DSB foams is a probable reason for the increase of foam stability.

293          The viscoelastic and compressing forces of the foams generated from the DSB

294      and EPS/DSB solutions with $C_{DSB}$ of 2 mM were detected by TA (Table S1,

295      Supporting information). The viscoelastic forces of the DSB and EPS/DSB foams are

296      approximately equal, while the compressing force of the EPS/DSB foam is larger than

297      that of the DSB foam, which demonstrates that the micro stiffness of the foam films is

298    enhanced[29] in the presence of EPS. The hyperbranched EPS molecules in the foam

299    film can prop up the foam films efficiently, which inspires an approach to achieving

300    extra-high foam stability.
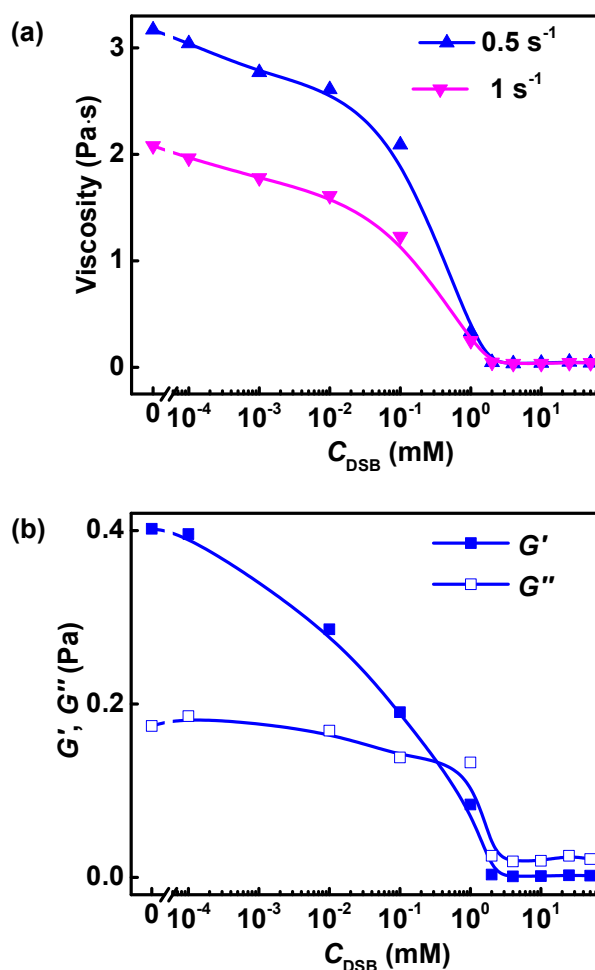


301



302

303    **Fig. 4** (a) Steady viscosity and (b) dynamic moduli ($G'$ and $G''$) of EPS/DSB

304    solutions with $C_{EPS}$ of 1.5 g/L as a function of $C_{DSB}$.

305

306    The bulk phase rheology of DSB and EPS/DSB solutions was also measured,

307    which is favorable for understanding the interactions between the EPS and the DSB.

308    The stress sweep curves indicates the existence of linear viscoelastic region for the

309    EPS and EPS/DSB solutions (Fig. S3, Supporting information). With increasing $C_{DSB}$,

310  both the steady viscosity and dynamic moduli increase till reaching the equilibrium

311  (Fig. 4). The DSB induced viscosity and dynamic modulus decreases of solutions are

312  caused by the co-aggregation of EPS and DSB molecules driven by the interactions

313  between them. On one hand, the DSB adsorbed on the EPS molecules acts as

314  hydrogen breakers which considerably disrupt the hydrogen bonds between EPS

315  molecules as shown in Fig. 2.[52-54] On the other hand, the cluster or micelle of the DSB

316  molecules formed on the EPS molecules can weaken the electric repulsion between

317  each other. The bulk rheological results further conform the interactions between the

318  EPS and the DSB.

319      Comparing the results in Fig. 4 with the results of foam stability shown in Fig. 1,

320  it is concluded that the steric repulsion caused by the association between the DSB

321  and the EPS plays an important role on the stability enhancement of the EPS/DSB

322  foam.[55]

323  *3.3 Foam drainage and coalescence of bubbles*
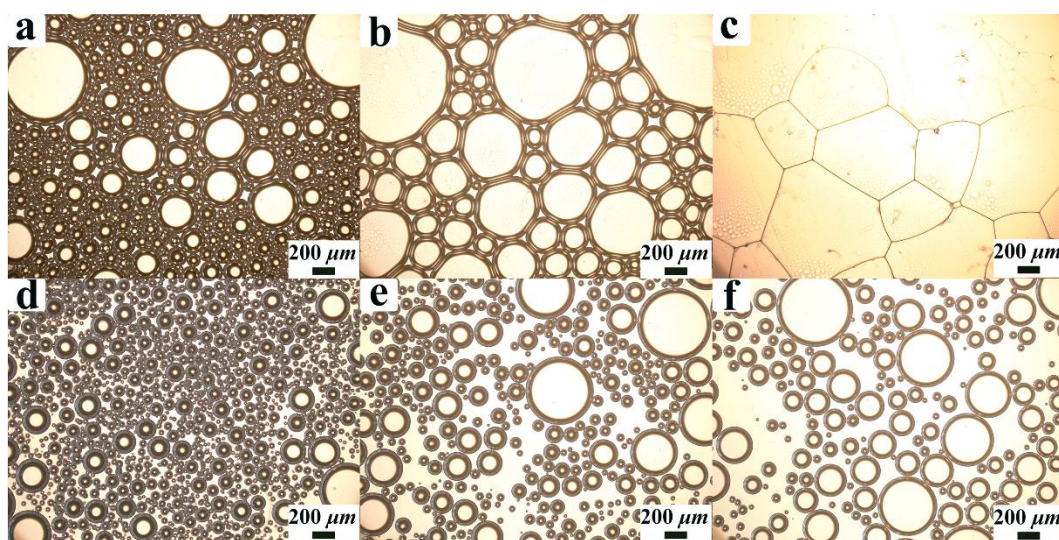


325

326  **Fig. 5** Microscope images of foam bubbles generated in (a–c) DSB and (d–f)

327     EPS/DSB solutions with $C_{DSB}$ of 2 mM (a, d) at the beginning of drainage and after

328     drainage for (b, e) 15 and (c, f) 30 min. $C_{EPS}$ is 0.75 g/L.

329

330        Fig. 5 shows the images of the foam bubbles generated in the DSB and EPS/DSB

331     solutions. The transformation of the bubbles with time shows clearly that the bubble

332     coalescence of the DSB foam was very quick, while that of the EPS/DSB foam was

333     very slow. The bubbles in the complex foam could last for 3.5 h (Fig. S4, Supporting

334     information), while that in the DSB foam disappeared in less than one hour, meaning

335     that Ostwald effect was highly restrained in the EPS/DSB foam.



336
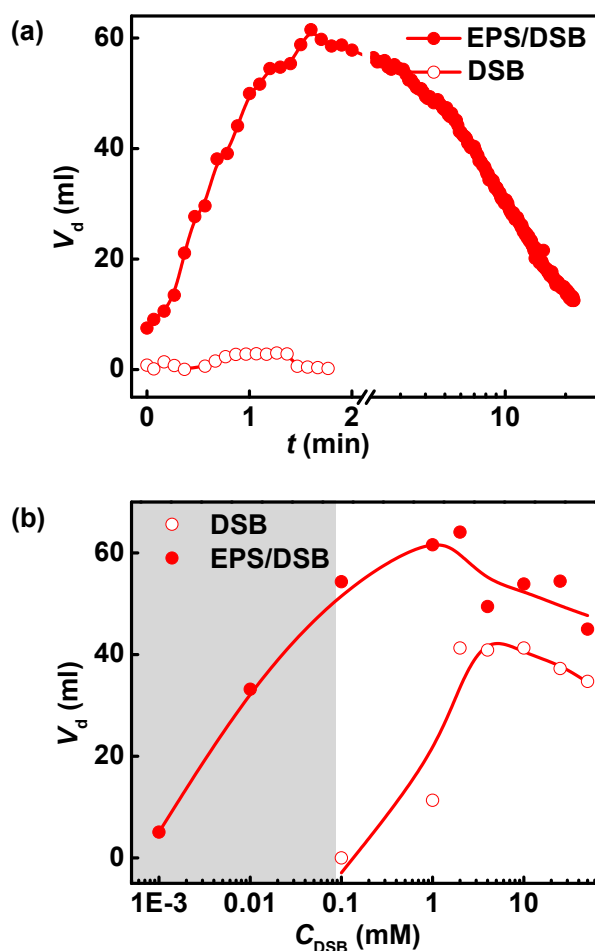


337

338     **Fig. 6** (a) Variation of liquid volume in DSB and EPS/DSB foams with time at $C_{DSB} =$

339    0.1 mM; (b) Liquid volume in DSB and EPS/DSB foams with different $C_{DSB}$ after

340    drainage for 100 s at 50 °C. $C_{EPS}$ is 1.5 g/L.

341

342        The time evolution of liquid volume ($V_d$) in the DSB and EPS/DSB foams was

343    monitored directly using Foamscan after the foam were generated. Fig. 6a shows the

344    time-dependence of the $V_d$ for DSB and EPS/DSB foams. The maximums of $V_d$ for

345    the EPS/DSB foam was ~30 times larger than that of the relative DSB foam, and Fig.

346    5 also shows that the water content in the EPS/DSB foam films (Fig. 5d–f) is higher

347    than that of pure DSB foams (Fig. 5a–c). Fig. 6b shows the liquid volumes in DSB

348    and EPS/DSB foams with different $C_{DSB}$ after drainage for 100 s. The EPS/DSB

349    foams have much stronger water-carrying capability than the pure DSB foams, which

350    probably arises from the strong hydrophilicity and hyperbranched structure of EPS.[22]

351    These results suggest that the EPS molecules entrapped inside the foam film is

352    capable of effectively inhibiting the coalescence of foam bubbles, and the increase of

353    water content in the foam films highly benefits the foam stability.

354    *3.4 Dynamic stability and rheological properties of DSB and EPS/DSB foams*
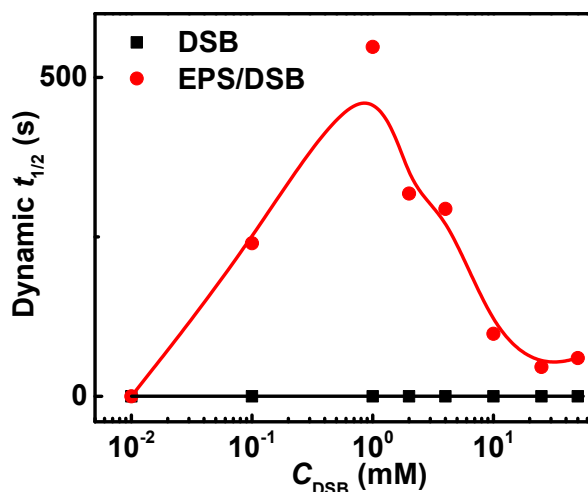


355

356    **Fig. 7** Dynamic half-life time of DSB and EPS/DSB foams at 50 °C as a function of

357    $C_{DSB}$ under shearing disturbance.

358

359    The dynamic stability of the foams, that is the stability under disturbance, was

360    also investigated. According to Fig. 7, at $C_{DSB}$ of $10^{-2}$–25 mM, the DSB foam can

361    hardly maintain the stability under shearing, while the dynamic $t_{1/2}$ of the EPS/DSB

362    foams is much longer in a very large $C_{DSB}$ range, indicating that the EPS/DSB foam

363    has a higher film strength under disturbance.[56, 57] Fig. 8a shows the change of

364    viscosity (10 s$^{-1}$) of EPS/DSB foams with time under shearing at 50 °C. The viscosity

365    of the EPS/DSB foams increases then decreases with time. Dynamic moduli of the

366    DSB and EPS/DSB foams with $C_{DSB}$ of 2 mM and $C_{EPS}$ of 1.5 g/L were measured, as

367    shown in Fig. 8b. The pure DSB foam exhibits high storage and loss moduli (*G'* and

368    *G"*) within initial several minutes, but decreases abruptly afterwards. The initial

369    increase of viscosity and dynamic moduli of foams with time is attributed to the

370    increase of the gas volume fraction of foams in the drainage process,[58] while the

371    subsequent decrease results mainly from bubble coalescence.[59, 60] The viscosity and

372    dynamic moduli of the EPS/DSB foam increases persistently and remains high in a

373    very long time (Fig. 8b), which indicates that the excellent water-carrying capacity is

374    very important for the good dynamic stability of the EPS/DSB foam, and the high

375    viscosity and elasticity of the liquid in the foam film caused by the EPS also

376    contribute to the good stability.
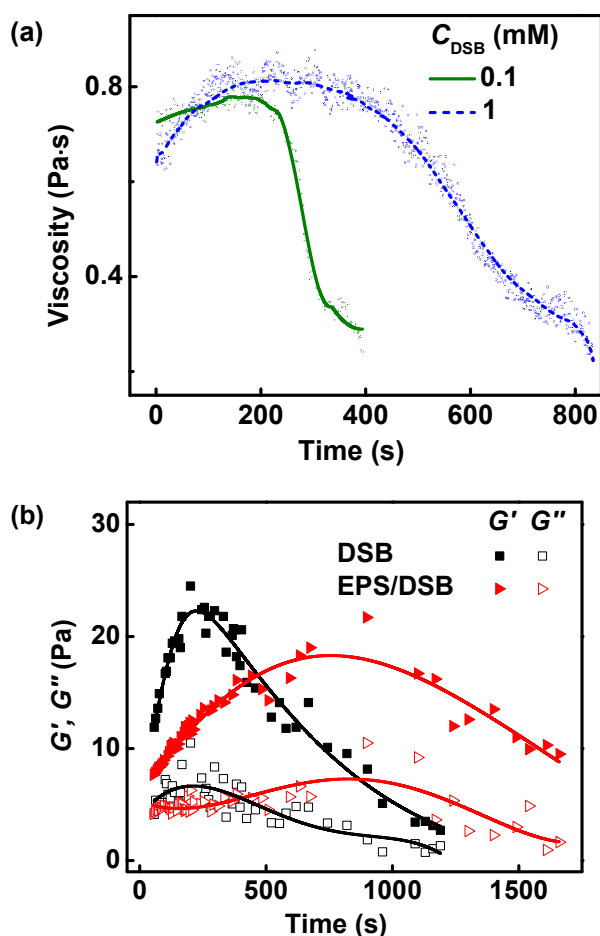
377



378

379 **Fig. 8** (a) Variations of apparent viscosity (10 s$^{-1}$) and (b) dynamic moduli of

380 EPS/DSB foams with time at $C_{DSB}$ = 2 mM, $C_{EPS}$ = 1.5 g/L and 50 °C.

381

382 *3.5 Effect of EPS concentration on foam properties*

383     Fig. 9a shows the $t_f$ and steady viscosity of EPS/DSB solutions at different $C_{EPS}$ and

384 $C_{DSB}$ = 2 mM. The $t_f$ and steady viscosity changes slightly at $C_{EPS}$ < ~1.0 g/L

385 approaching to the overlapping concentration of the EPS (0.95 g/L),[23] and

386 prominently increases at $C_{EPS}$ > ~1.0 g/L with increasing $C_{EPS}$. The increase of $t_f$

387 results from the increase of the steady viscosity because the increase of the viscosity

388 is unfavorable for the adsorption of the surfactant molecules at gas/water interface and

389 the development of gas bubbles.[34, 35]

390



391
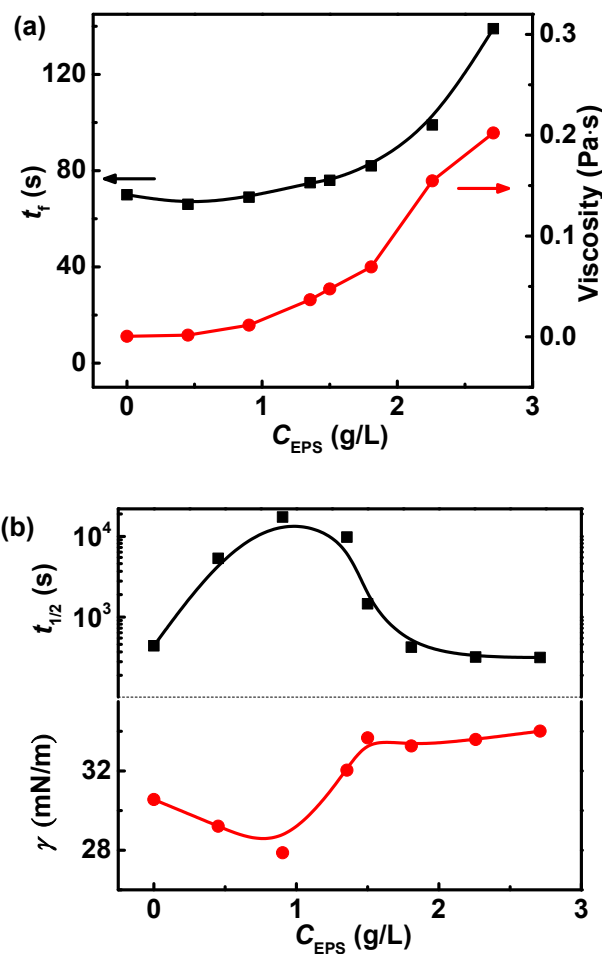
**Fig. 9** (a) Foaming times ($t_f$), (a) steady viscosity at 0.5 s$^{-1}$ and (b) surface tension ($\gamma$)

of EPS/DSB solutions and (b) half-life times ($t_{1/2}$) of EPS/DSB foams as a function of

$C_{EPS}$ at $C_{DSB}$ = 2 mM.


As shown in Fig. 9b, the $t_{1/2}$ of the EPS/DSB foams at $C_{DSB}$ = 2 mM increases at

$C_{EPS}$ < 1 g/L, and then decreases with increasing $C_{EPS}$. The maximum $t_{1/2}$ is observed

at $C_{EPS}$ = 1 g/L. According to the discussion in section 3.1 and 3.2, the formation of

the EPS/DSB complex enhances the foam stability. The variation of the surface

tension obtained from the dynamic surface tension curves (Fig. S5, supporting

information) of the EPS/DSB solutions as a function of $C_{EPS}$ at $C_{DSB}$ = 2 mM is also

402    shown in Fig. 9b. The adsorption of EPS and DSB complex at $C_{EPS} < 1$ g/L benefits

403    the decrease of the surface tension and brings positive effect on the foam stability. At

404    $C_{EPS}$ larger than the overlapping concentration, EPS molecules are prone to form

405    associations through hydrogen bonds in the bulk instead of forming EPS/DSB

406    complex in the interfacial layer, which makes the amount of the EPS/DSB complex at

407    the interface decrease, the surface tension increase, and the foam stability decrease.

408    Thus, there is an optimal concentration for EPS to enhance the foamability and foam

409    stability of surfactants. This optimal concentration should be lower than its

410    overlapping concentration.

411    **4. Conclusions**

412    An eco-friendly complex solutions containing DSB and a hyperbranched

413    polysaccharide EPS which have weak interactions was found to be an effective

414    foaming system. The minimum $C_{DSB}$ in the EPS/DSB foams needed for the formation

415    of foams decreased ~100 times than that in the relative DSB foams, and the foam

416    stability enhanced more than ten times in the presence of EPS. The enhanced

417    foamability resulted from the increase of the interfacial adsorption tendency of DSB

418    caused by the EPS induced change of water properties. The EPS/DSB foam stability

419    is highly related to its interfacial elasticity and water-carrying ability enhanced by the

420    formation of EPS/DSB molecular networks at the interface through hydrogen bonds

421    and electrostatic attraction force between them. The hyper-branched structure and

422    high hydrophilic character of EPS resist disturbance and deformation of the foam film,

423    which benefits a lot on the enhancement of the complex foam stability. This work

424    provides a deep insight into the mechanism of performance enhancement of

PE/surfactant complex foam with weak interactions, which can be a very useful

approach to exploring eco-friendly high efficient foam systems.

**References**

1.  A. Aziz, H. C. Hailes, J. M. Ward and J. R. G. Evans, *RSC Adv.*, 2014, **4**(95), 53028-53036.

2.  O. Arjmandi-Tash, N. Kovalchuk, A. Trybala and V. Starov, *Soft matter*, 2015, **11**(18), 3643-3652.

3.  D. Y. C. Chan, E. Klaseboer and R. Manica, *Soft Matter*, 2011, **7**(6), 2235-2264.

4.  C. Üzüm, N. Kristen and R. von Klitzing, *Curr. Opin. Colloid Interface Sci.*, 2010, **15**(5), 303-314.

5.  R. V. Klitzing, A. Espert, A. Asnacios, T. Hellweg, A. Colin and D. Langevin, *Colloids Surf. A*, 1999, **149**(1–3), 131-140.

6.  R. Petkova, S. Tcholakova and N. D. Denkov, *Langmuir*, 2012, **28**(11), 4996-5009.

7.  A. Bureiko, A. Trybala, N. Kovalchuk and V. Starov, *Adv. Colloid Interface Sci.*, 2014, DOI:10.1016/j.cis.2014.10.001.

448    8.    L. Xu, G. Xu, H. Gong, M. Dong, Y. Li and Y. Zhou, *Colloids Surf. A*, 2014,

449         **456**(0), 176-183.

450    9.    H. Ritacco, P.-A. Albouy, A. Bhattacharyya and D. Langevin, *Phys. Chem.*

451         *Chem. Phys.*, 2000, **2**(22), 5243-5251.

452    10.   C. Monteux, G. G. Fuller and V. Bergeron, *J. Phys. Chem. B*, 2004, **108**(42),

453         16473-16482.

454    11.   B. Jean, L.-T. Lee, B. Cabane and V. Bergeron, *Langmuir*, 2008, **25**(7),

455         3966-3971.

456    12.   W. Lv, Y. Li, Y. Li, S. Zhang, Q. Deng, Y. Yang, X. Cao and Q. Wang, *Colloids*

457         *Surf. A*, 2014, **457**(0), 189-195.

458    13.   S. Xu, Z. Bai, B. Jin, R. Xiao and G. Zhuang, *Sci. Rep.*, 2014,

459         DOI:10.1038/srep04131.

460    14.   M. Ropers, B. Novales, F. Boué and M. A. Axelos, *Langmuir*, 2008, **24**(22),

461         12849-12857.

462    15.   T. Brenner, R. Tuvikene, A. Parker, S. Matsukawa and K. Nishinari, *Food*

463         *Hydrocolloids*, 2014, **39**(0), 272-279.

464    16.   H. Li, H. Xu, S. Li, X. Feng, H. Xu and P. Ouyang, *Process. Biochem.*, 2011,

465         **46**(5), 1172-1178.

466    17.   X. T. Le and S. L. Turgeon, *Soft Matter*, 2013, **9**(11), 3063-3073.

467    18.   J. P. Osano, S. H. Hosseini-Parvar, L. Matia-Merino and M. Golding, *Food*

468         *Hydrocolloids*, 2014, **37**(0), 40-48.

469    19.   F. L. Jara, C. Carrera Sánchez, J. M. Rodríguez Patino and A. M. R. Pilosof,

470      *Food Hydrocolloids*, 2014, **35**(0), 189-197.

471    20.    Q.-L. Qin, D.-L. Zhao, J. Wang, X.-L. Chen, H.-Y. Dang, T.-G. Li, Y.-Z.

472      Zhang and P.-J. Gao, *FEMS Microbiol. Lett.*, 2007, **271**(1), 53-58.

473    21.    W. Zhou, J. Wang, B. Shen, W. Hou and Y. Zhang, *Colloids Surf. B*, 2009,

474      **72**(2), 295-302.

475    22.    H. Li and W. Hou, *Food Hydrocolloids*, 2011, **25**(6), 1547-1553.

476    23.    H. Li, W. Hou and Y. Zhang, *Carbohydr. Polym.*, 2011, **84**(3), 1117-1125.

477    24.    N. Kamenka, Y. Chevalier and R. Zana, *Langmuir*, 1995, **11**(9), 3351-3355.

478    25.    J. Zajac, C. Chorro, M. Lindheimer and S. Partyka, *Langmuir*, 1997, **13**(6),

479      1486-1495.

480    26.    V. Seredyuk, E. Alami, M. Nydén, K. Holmberg, A. V. Peresypkin and F. M.

481      Menger, *Langmuir*, 2001, **17**(17), 5160-5165.

482    27.    L. Qi, Y. Fang, Z. Wang, N. Ma, L. Jiang and Y. Wang, *J. Surfactants Deterg.*,

483      2008, **11**(1), 55-59.

484    28.    Z. Li, H. Yan, X. Song, S. Yuan, B. Pan and L. Wang, *Acta Chim. Sinica.*, 2011,

485      **69**(8), 898-904.

486    29.    X. Y. Hu, Y. Li, X. J. He, C. X. Li, Z. Q. Li, X. L. Cao, X. Xin and P.

487      Somasundaran, *J. Phys. Chem. B*, 2012, **116**(1), 160-167.

488    30.    R. Petkova, S. Tcholakova and N. D. Denkov, *Colloids Surf. A*, 2013, **438**(0),

489      174-185.

490    31.    E. Carey and C. Stubenrauch, *J. Colloid Interface Sci.*, 2010, **346**(2), 414-423.

491    32.    N. Kristen, A. Vüllings, A. Laschewsky, R. Miller and R. von Klitzing,

492        *Langmuir*, 2010, **26**(12), 9321-9327.

493    33.    V. Bergeron, D. Langevin and A. Asnacios, *Langmuir*, 1996, **12**(6),

494        1550-1556.

495    34.    B. M. Folmer and B. Kronberg, *Langmuir*, 2000, **16**(14), 5987-5992.

496    35.    R. Farajzadeh, R. Krastev and P. L. J. Zitha, *Langmuir*, 2009, **25**(5),

497        2881-2886.

498    36.    V. Carrier and A. Colin, *Langmuir*, 2003, **19**(11), 4535-4538.

499    37.    S. Tcholakova, Z. Mitrinova, K. Golemanov, N. D. Denkov, M. Vethamuthu

500        and K. P. Ananthapadmanabhan, *Langmuir*, 2011, **27**(24), 14807-14819.

501    38.    M. M. Il'in, M. S. Anokhina, M. G. Semenova, L. E. Belyakova and Y. N.

502        Polikarpov, *Food Hydrocolloids*, 2005, **19**(3), 441-453.

503    39.    B. S. Murray, *Curr. Opin. Colloid Interface Sci.*, 2007, **12**(4), 232-241.

504    40.    M. S. Anokhina, M. M. Il'In, M. G. Semenova, L. E. Belyakova and Y. N.

505        Polikarpov, *Food Hydrocolloids*, 2005, **19**(3), 455-466.

506    41.    H. Fruhner, K. D. Wantke and K. Lunkenheimer, *Colloids Surf. A*, 1999,

507        **162**(1–3), 193-202.

508    42.    P. Deo and P. Somasundaran, *Langmuir*, 2005, **21**(9), 3950-3956.

509    43.    G. Zhao, C. C. Khin, S. B. Chen and B.-H. Chen, *J. Phys. Chem. B*, 2005,

510        **109**(29), 14198-14204.

511    44.    L. Gřundělová, A. Gregorova, A. Mráček, R. Vícha, P. Smolka and A. Minařík,

512        *Carbohydr. Polym.*, 2015, **119**(0), 142-148.

513    45.    J. H. Kim, B. R. Min, K. B. Lee, J. Won and Y. S. Kang, *Chem. Commun.*,

514       200222), 2732-2733.

515   46.   C. Zhong and P. Luo, *J. Polym. Sci. Poly. Phys.*, 2007, **45**(7), 826-839.

516   47.   K. Saadati, K. Kabiri and G. B. Marandi, *Int.J. Polym.Mater.*, 2014, **63**(8),

517       430-437.

518   48.   D. J. F. Taylor, R. K. Thomas, J. D. Hines, K. Humphreys and J. Penfold,

519       *Langmuir*, 2002, **18**(25), 9783-9791.

520   49.   A. Bhattacharyya, F. Monroy, D. Langevin and J.-F. Argillier, *Langmuir*, 2000,

521       **16**(23), 8727-8732.

522   50.   D. P. Acharya, J. M. Gutiérrez, K. Aramaki, K.-i. Aratani and H. Kunieda, *J.*

523       *Colloid Interface Sci.*, 2005, **291**(1), 236-243.

524   51.   E. Manev, A. Scheludko and D. Exerowa, *Colloid Polym. Sci.*, 1974, **252**(7-8),

525       586-593.

526   52.   E. Kokufuta, H. Suzuki, R. Yoshida, K. Yamada, M. Hirata and F. Kaneko,

527       *Langmuir*, 1998, **14**(4), 788-795.

528   53.   D. Corradini, *J. Chromatogr. B: Biomed. Appl.*, 1997, **699**(1–2), 221-256.

529   54.   A. Jakubowska, *J. Colloid Interface Sci.*, 2010, **346**(2), 398-404.

530   55.   A. Cervantes-Martínez and A. Maldonado, *J. Phys:condens. Mat.*, 2007,

531       **19**(24), 246101-246108.

532   56.   A. Bureiko, A. Trybala, J. Huang, N. Kovalchuk and V. Starov, *Colloids Surf.*

533       *A*, 2014, **460**(0), 265-271.

534   57.   K. D. Martínez, M. E. Farías and A. M. R. Pilosof, *Food Hydrocolloids*, 2011,

535       **25**(7), 1667-1676.

536 58. C. A. Jimenez-Junca, J. C. Gumy, A. Sher and K. Niranjan, *J. Food Sci.*, 2011,

537 **76**(9), E569-E575.

538 59. K. Bekkour and O. Scrivener, *Mechanics Time-Dependent Materials*, 1998,

539 **2**(2), 171-193.

540 60. S. D. P. Eugénie, D. Fabrice, C. Gérard and M. Samir, *Food Hydrocolloids*,

541 2014, **34**(0), 104-111.

542